5D.6 EASTERLY WAVE STRUCTURAL EVOLUTION OVER WEST AFRICA AND THE EAST ATLANTIC

Matthew A. Janiga*
University at Albany, Albany, NY

1. INTRODUCTION

African easterly waves (AEWs) are synoptic-scale disturbances which develop over the African continent during the monsoon. Fink and Reiner (2003) noted a strong preference for squall lines to be observed to the northwest of the mid-level vorticity maxima associated with AEWs. However, what determines the relationship between convection and AEWs and how this relates to the evolution of the AEW is not well understood.

To address this question we examine the relationship between convection and AEWs in a composite long-lived AEW. This is done by creating a vortex-centered composite of the progression of 64 long-lived AEWs between 5ºE and 20ºW. Gridded fields from the European Center for Medium Range Weather Forecasting (ECMWF) Interim Reanalysis (ERA-Interim) and infrared brightness temperature data from the CLoud User Archive Service (CLAUS) dataset (Hodges et al., 2000) were composited relative to the mid-level vortex center of these 64 long-lived AEWs.

To examine the relationship between convection and the AEWs we examine the how the distribution of lift, moisture, and instability are modified by the composite AEW as it progresses from West Africa to the East Atlantic. To provide context for the evolving relationship between the AEW and convection between West Africa and the East Atlantic the dynamical evolution of the AEW is also examined.

2. COMPOSITE GENERATION

Thorncroft and Hodges (2001) examined the tracks of 600 and 850 hPa vorticity maxima exceeding 0.5×10^{-5} s^{-1} on T42 (~500 km grid resolution) analyses with lifetimes exceeding 2 days and a westward propagation exceeding 10º. The track density of the mid-level disturbances was greatest west of 10ºE and near 10ºN corresponding to the location of the mid-level potential vorticity (PV) strip. The low-level disturbances were found near 20ºN between 0ºE-15ºW over the African continent and at 10ºN over the ocean.

So that the objective AEW positions represent the movement of the synoptic-scale mid-level circulation and are not significantly influenced by short-lived mesoscale vorticity anomalies (e.g. Berry and Thorncroft, 2005) we first reduced the effective resolution of the 1.5 ERA-Interim analyses. First the 700 hPa vorticity was averaged within a 4.5º radius of each grid point resulting in an approximately 1000 km resolution measure of the mid-level circulation. Then the circulation was 2-day low pass filtered to remove short-lived featuers.

Mid-level circulation maxima within a 9º radius exceeding 1×10^{-5} s^{-1} were tracked by extrapolating their expected position after initial identification and matching it to maxima identified at the following time within a 7.5º radius of their extrapolated position. The tracking program was tuned to highlight those disturbances which are unambiguous on Hövmoller diagrams and plan maps even in high resolution analyses.

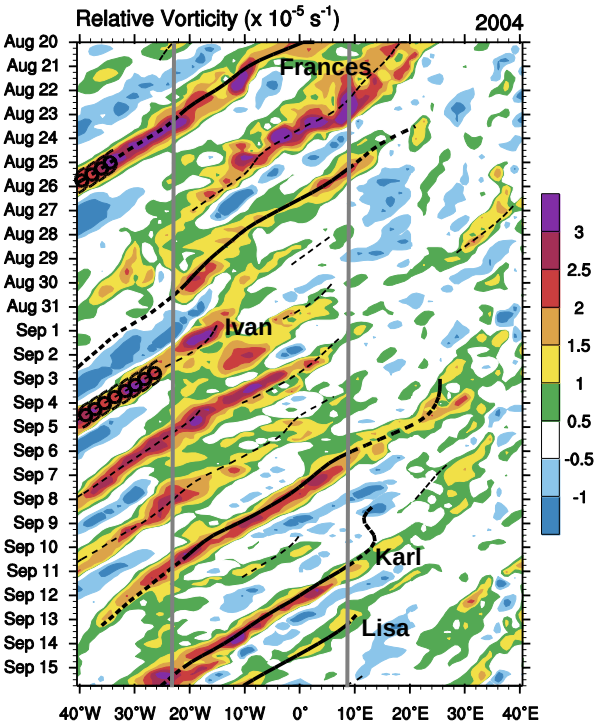

FIG. 1. Hovmoller of 700 hPa relative vorticity with overlayed objective tracks. Qualified (unqualified) tracks are thick (thin and dashed). Those qualified tracks in the compositing domain (7.5E-22.5W) are thick.

These tracks are further filtered for those disturbances which have a continuous track between 7.5ºE and 22.5ºW and between 0-20ºN and occur during the period of July-September, 1989-2005. Composites were produced at 5º intervals (5ºE, 0º, 5ºW, 10ºW, 15ºW, 20ºW) with 5º width bins by compositing

* *Corresponding author address:* Matthew A. Janiga, Univ. at Albany, Dept. of Atmospheric and Environmental Science, Albany, NY 12222; e-mail: janiga@atmos.albany.edu.

ERA-Interim and CLAUS grids via a vortex centered approach.

Fig. 1 shows a Hövmoller diagram of 700 hPa relative vorticity with qualified tracks indicated by thick lines and unqualified tracks by thin lines. During this period five tracks (including the AEWs associated with Hurricane Frances, Karl, and Lisa) were selected for compositing. Some tracks were disqualified because of a track break or because the disturbance didn't form far enough east or traverse far enough west. However, this work only addresses the generation and analysis of a coherent composite evolution of AEWs and not a climatology of all disturbances.

3. COMPOSITE ANALYSIS

Two factors are at work in modifying the structure and relationship with convection of AEWs as they progress from east to west across the six geographic compositing bins. The first is the change in basic state fields such as low-level baroclinicity, vertical wind shear, and convective available potential energy (CAPE) between West Africa and the East Atlantic. Another factor is the evolution in time and growth of the disturbances. Fig. 2 shows a box-and-wisker plot of the distribution of track ages in each of the geographic bins. The 5ºE and 20ºW composite AEWs have a median track age of 3 and 6.5 days, respectively. The median zonal velocity of the composited disturbances is about -9 ms^{-1} between the 5ºE-15ºW bins decreasing to -7 ms^{-1} in the 20ºW bin.

Fig. 3 shows the evolution of the mid-level (PV) strip in the composite AEW at 5.0ºE and 20.0ºW. At 5.0ºE the AEW trough axis, as indicated by the streamfunction contours south of the PV strip has a southwest to northeast tilt. At this time the 700 hPa PV is characterized by an anomaly embedded in a fairly zonal strip. By 20.0ºW the center of the mid-level vortex is slightly farther north and PV is characterized by a pronounced wave in addition to an embedded PV

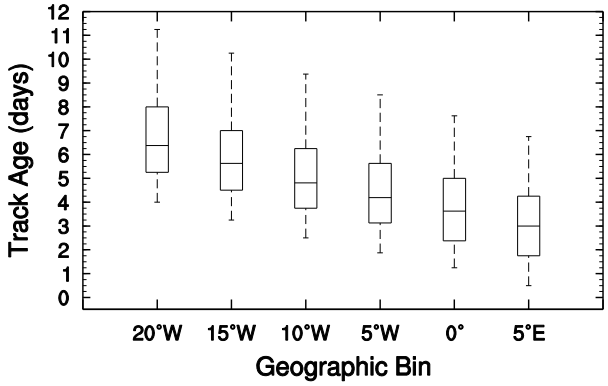

FIG. 2. Box and wisker plot (5th, 25th, 50th, 75th, and 95th percentiles) of the vortex ages (days) used to construct the composite for each of the six geographic bins.

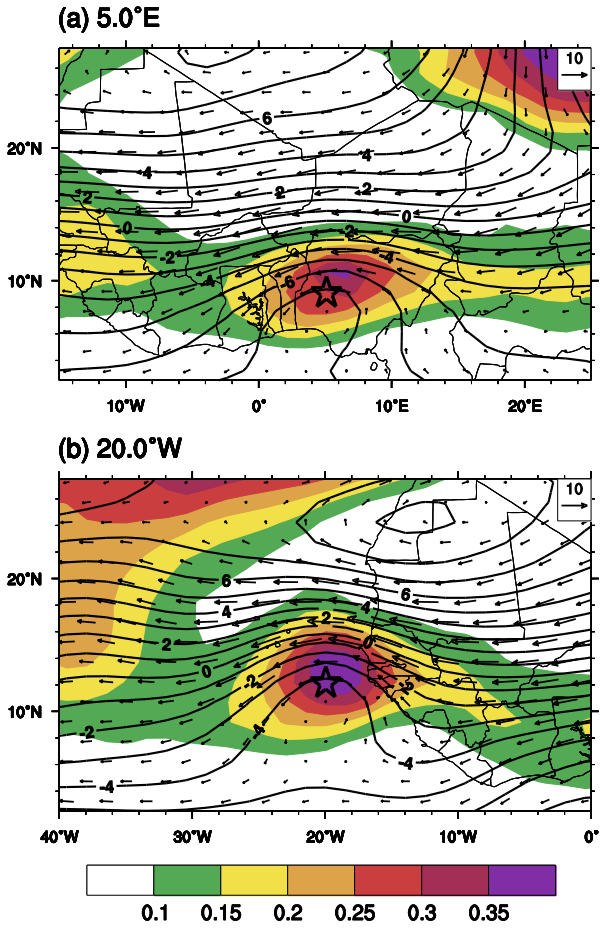

FIG. 3. 700 hPa potential vorticity (PVU, shaded), streamfunction (x10^6 m^2s^{-1}, contours), and winds (ms-1) for the (a) 5.0°E and (b) 20°W composite bins. The average position of the composited mid-level vortices is indicated by a star.

anomaly. The tilt of the AEW trough is reduced as the AEW moves westward consistent with barotropic growth at the expense of the basic state. Recall that the mid-level vortex position used for generating the composites is taken from the maxima of vorticity averaged about a 4.5º radius and so does not necessarily have to be exactly collocated with the highest mid-level PV in the 1.5º composited ERA-Interim fields.

Low-level vortices are frequently observed to the northwest of the mid-level AEW vortex along the ITD. Carlson (1969) proposed that the northerly flow over the ITD induced by the mid-level AEW vortex would induce a positive potential temperature anomaly and a resulting cyclonic circulation. To understand the evolution of the low-level moisture and other convective ingredients it is important to understand how this baroclinic growth influences the evolution of the low-level structure of the AEWs.

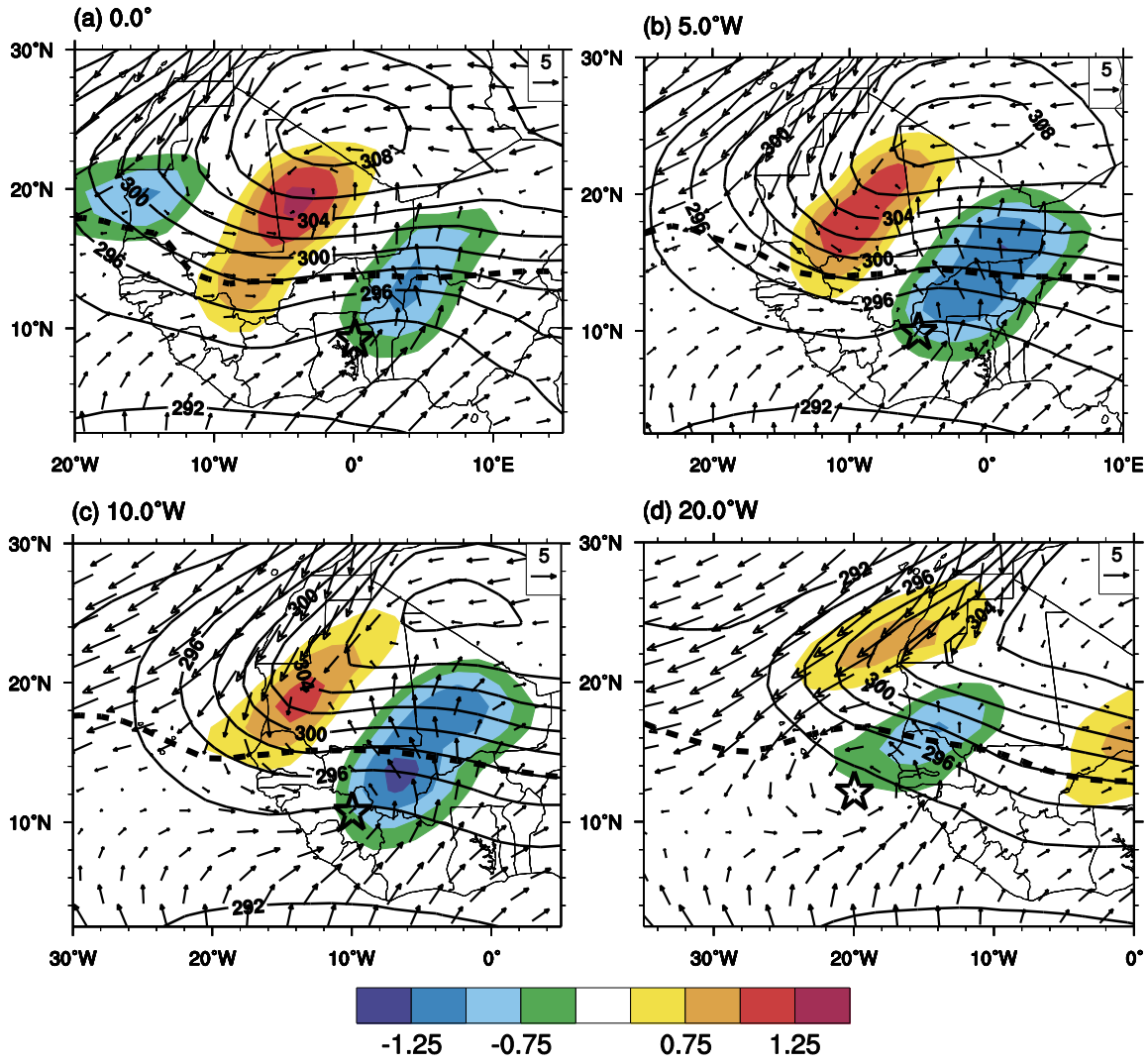

FIG. 4. 925 hPa potential temperature (contours, K), 2-10 day filtered temperature (shaded, K), and wind (vectors) for the (a) 0ºE, (b) 5ºW, (c) 10ºW, and (d) 20ºW AEW composites. The composite 700 hPa vortex positions and African easterly jet (AEJ) are indicated by a star and thick dashed line, respectively.

Fig. 4 shows the low-level wind field and potential temperature in four geographic bins. To highlight the temperature anomalies the composite 2-10 day bandpass filtered potential temperature is shaded. For the 0ºE composite a cyclonic circulation and a positive potential temperature anomaly are observed at 19ºN, 5ºW. Moving toward the west coast of Africa the east-west tilt between the northern vortex and the mid-level vortex decreases and the temperature anomalies become elongated about a southwest to northeast axis. This can be understood as a response to the change in the basic state temperature gradient orientation from zonal at 0ºE to meridional, and unfavorable for baroclinic growth, at 20ºW.

The 2-10 day filtered relative vorticity and wind at 925 hPa are shown in Fig. 5. At 0ºE the positive potential temperature perturbation to the north is coincident with a low-level vortex. A cross-section through this vortex reveals that it weakens with height disappearing near 700 hPa which is also the depth where the meridional temperature gradient reverses and baroclinic growth can no longer occur. A low level cold-core anticyclone is observed to the northeast of the mid-level vortex and also extends to 700 hPa. In the composites further west the northern vortex becomes elongated about a southwest to northeast axis consistent with the previously mentioned elongation of the potential temperature anomalies in response to the changing low-level basic state temperature gradients. Another cause of this elongation may be deformation induced by the interaction of the northern-vortex with the anticyclone to the east and the cyclonic circulation beneath the mid-level vortex to the south.

By 20ºW there are no longer two distinct cyclonic circulations at 925 hPa. At this longitude the mid-level vortex is still able to grow through diabatic processes and induce a stronger and stronger circulation at the surface. Meanwhile the northern vortex is no longer able grow baroclinically and is experiencing continued deformation.

Fig. 6 shows the evolution of convection relative to the mid-level vortex. Convection is represented by the percentage of grids which exceed the 208K brightness temperature threshold in the CLAUS dataset. The convection is located to the northwest of the mid-level vortex in each of the geographic bins but the one at 20ºW which has convection maximized to the southwest. In the 5ºE composite the convection is greatest along a southwest to norheast axiz. At 5ºW and 10ºW the convection appears to be more tightly clustered in the northwest quadrant. At 15ºW the convection is highly compacted but remains northwest of the mid-level vortex.

In an attempt to approximate the balanced forcing for ascent we calculate the 700-900 hPa mean layer Q vectors and their convergence. Since the geostrophic wind is a poor approximation for the balanced flow at this latitude we instead use the non-divergent wind and define Q_1 and Q_2 following Kiladis et al. (2006).

$$Q_1 \equiv -\frac{R}{p}\frac{\partial V_\psi}{\partial x}\nabla\cdot\mathbf{T} = -\frac{R}{p}\left(\frac{\partial u_\psi}{\partial x}\frac{\partial T}{\partial x}+\frac{\partial v_\psi}{\partial x}\frac{\partial T}{\partial y}\right), \quad (1)$$

$$Q_2 \equiv -\frac{R}{p}\frac{\partial V_\psi}{\partial y}\nabla\cdot\mathbf{T} = -\frac{R}{p}\left(\frac{\partial u_\psi}{\partial y}\frac{\partial T}{\partial x}+\frac{\partial v_\psi}{\partial y}\frac{\partial T}{\partial y}\right), \quad (2)$$

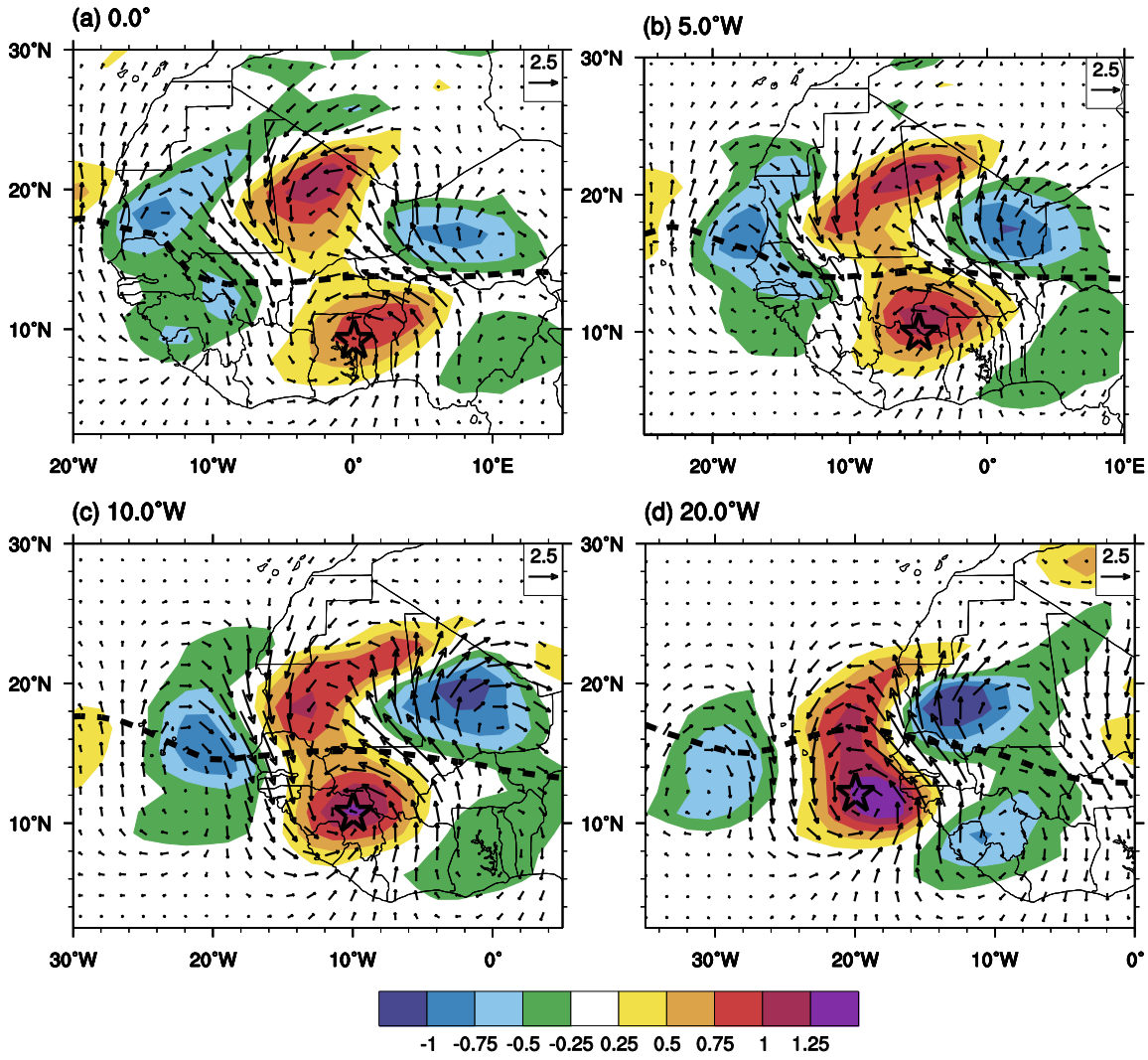

FIG. 5. 2-10 day filtered relative vorticity (x10^{-5} s^{-1}, shaded) and wind (ms^{-1}, vectors) at 925 hPa for the (a) 0ºE, (b) 5ºW, (c) 10ºW, and (d) 20ºW AEW composites.

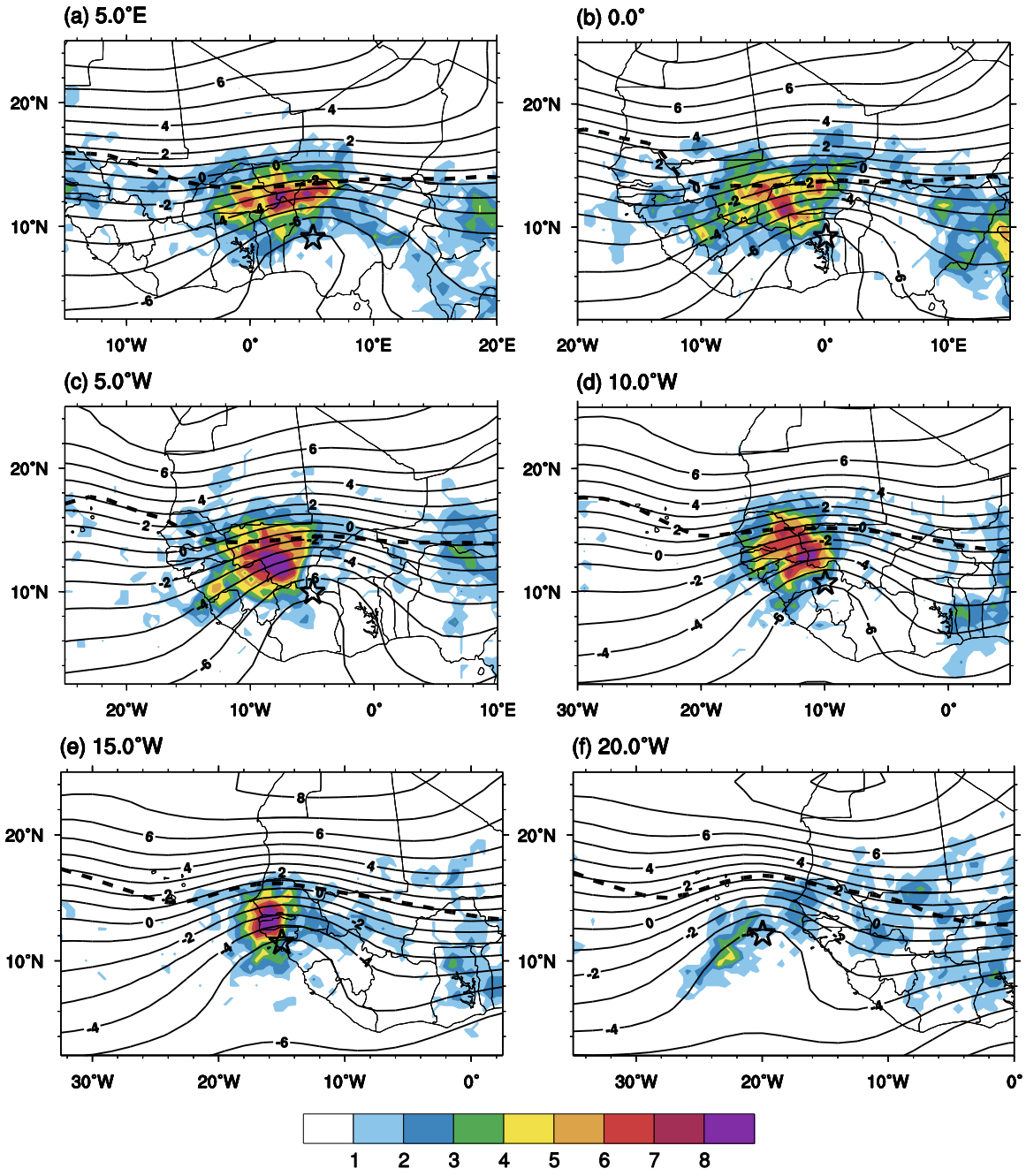

FIG. 6. 700 hPa streamfunction ($x10^6 m^2 s^{-1}$, contours), and the percentage of composited grids which exceeded an infrared brightness temperature of 208K (%, shaded) for the (a) 5ºE, (b) 0ºE (c) 5ºW, (d) 10ºW, (e) 15ºW, and (f) 20ºW AEW composites.

In the 5ºW composite the Q vector convergence is maximized to the northwest of the mid-level vortex (Fig. 7) as would be expected since the mid-level AEJ and low-level temperature gradient are strongest north of the mid-level vortex. A second Q vector convergence maxima is observed to the west of the northern vortex and is associated with low-level ascent in composites of the ERA-Interim vertical velocity (not shown). Q vector convergence and convection are collocated northwest of the mid-level vortex in the other geographic composites.

The fact that convection isn't occurring everywhere or to the northeast of the mid-level vortex where there is Q vector divergence implies that forcing for ascent may be an important factor for the development of moist convection associated with AEWs. This is likely due to the large values of CAPE and convective inhibition (CIN) in the semi-arid Sahel (Fig. 8).

Fig. 9a shows that despite their being perturbation northerlies at low-levels northwest of the AEW mid-level vortex the unfiltered wind is from the west and moist. It is not until the AEWs reach 15ºW and 20ºW that dry low-level air is found northwest of the AEW mid-level vortex (Fig. 9b). This dry air may be responsible for the compactness of the convective maxima at 15ºW (Fig. 6e) and the shift of the convection to southwest of the mid-level vortex at 20ºW (Fig. 6f)

In summary convection associated with AEWs has a strong relationship with low-level Q vector convergence. This provides the motivation for calculating the magnitude of the vertical motion associated with the balanced flow possibly under the assumption of non-linear balance. Low-level moisture appears to be a necessary condition as well. Case studies using higher resolution analyses or numerical models could be used to more closely examine the trajectories of the moist unstable air that feeds the moist convection to the northwest of the mid-level vortex.

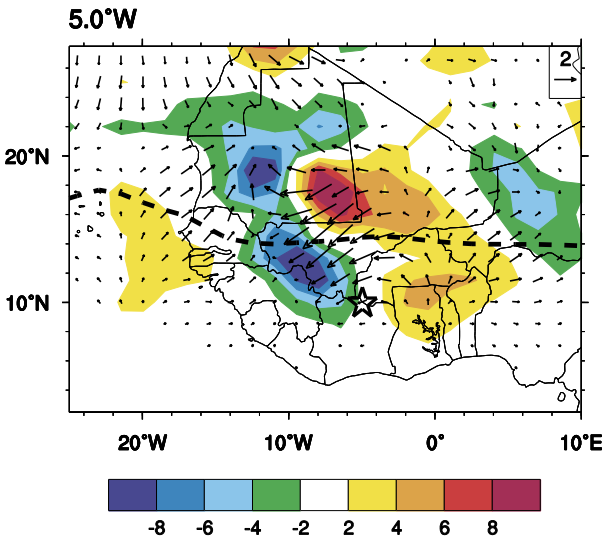

FIG. 7. 700-900 mean-layer Q-vectors (x 10^{-14} $mPa^{-1}s^{-3}$, vectors) and Q-vector convergence (x 10^{-19} $Pa^{-1}s^{-3}$, shaded) for the 5ºW AEW composite.

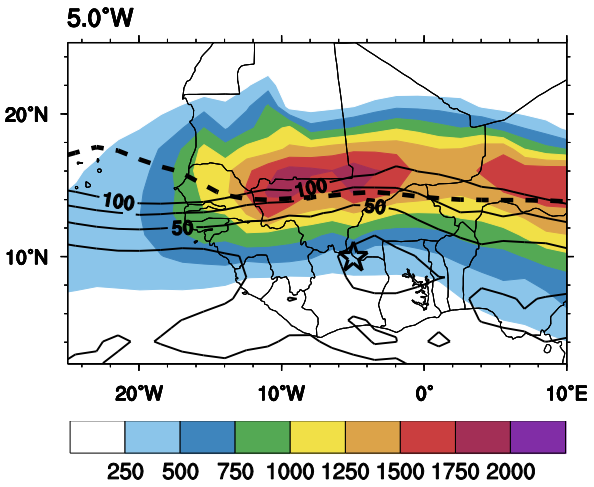

FIG. 8. CAPE (J kg-1, shaded) and CIN (J kg^{-1}, contours) for the AEW composite

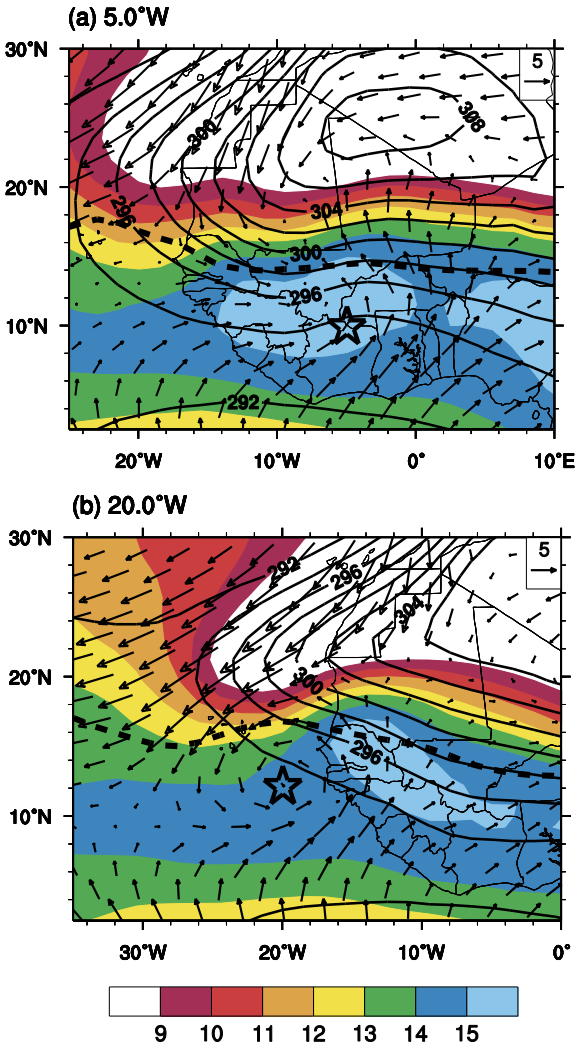

FIG. 9. 925 hPa potential temperature (K, shaded), mixing ratio (gkg^{-1}, shaded), and wind (ms^{-1}, vectors) for the (a) 5ºW and (b) 20ºW AEW composites.

REFERENCES

Berry, G. J. and C. Thorncroft. 2005. Case study of an intense African easterly wave. Mon. Wea. Rev. 133:752–766.

Carlson, T. N., 1969: Some remarks on African disturbances and their progress over the tropical Atlantic. *Mon. Wea. Rev.,* **97,** 716–726.

Fink, A. H. and A. Reiner, 2003: Spatiotemporal variability of the relation between African Easterly Jets and and West African Squall lines in 1998 and 1999. *J. Geophys. Res.*, **108**.4332, doi:10.1029/2002JD002816.

Hodges, K. I., D. W. Chappell, G. J. Robinson, and G. Yang, 2000: An improved algorithm for generating global window brightness temperatures from multiple satellite infrared imagery. *J. Atmos. Oceanic Technol.*, **17**:1296–1312.

Kiladis, G. N., C. D. Thorncroft, and N. G. Hall, 2006: Three-dimensional structure and dynamics of African easterly waves. Part I: Observations. *J. Atmos. Sci.*, **63**:2212–2230.

Thorncroft, C. D. and K. Hodges, 2001: African easterly wave variability and its relationship to Atlantic tropical cyclone activity. *J. Climate*, **14**:1166–1179.